I&EC research
Industrial & Engineering Chemistry Research

Article

pubs.acs.org/IECR

Continuous-Flow Aqueous System for Heterogeneous Photocatalytic Disinfection of Gram-Negative *Escherichia coli*

Mejdi Kacem,[†,‡] Gael Plantard,[†,‡] Monica Brienza,[†] and Vincent Goetz*[,†]

[†]PROMES CNRS, UPR 8521, Rambla de la thermodynamique, 66100 Perpignan, France
[‡]University of Perpignan Via Domitia, 52 Paul Alduy, 66100 Perpignan, France

ABSTRACT: Within the global objective to develop a sustainable oxidative process based on heterogeneous photocatalysis, the possibility of combining solar UV irradiation and a supported semiconductor all while working in an open reactor running in continuous flow is a pertinent option. Here we investigated a heterogeneous photocatalytic disinfection process performed with a 2D-photocatalytic material implemented in an open-flow flat-plate reactor irradiated with a LED panel. Inactivation of Gram-negative *Escherichia coli* was attempted using different UV light flux densities and feed flow rates. Treatment capacities were calculated under steady-state conditions using a simple mass balance between inlet and outlet. For an irradiated surface of 1.5×10^{-2} m^2, values ranged from 10 to 30×10^5 MPN h^{-1} L^{-1}as a function of working conditions. With just a few adjustments, the model based on coupling mass transfer with phototocatalysis-driven bacterial inactivation developed previously in the case of a closed-batch cylindrical reactor was tested and extended with success.

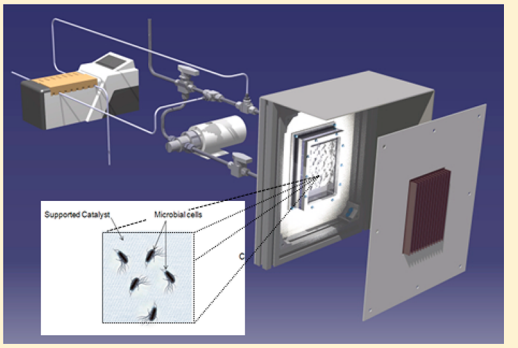

1. INTRODUCTION

Water-related problems are increasingly recognized as one of the most serious and immediate environmental threats to humankind. Numerous approaches exist throughout the world to promote wastewater reuse, especially in agriculture.[1] Urban wastewater is forwarded to treatment plants (WWTP), which are a set of devices (primary treatment devices followed by a secondary biological treatment) designed to progressively treat different pollutants. Recent station yields can reach up to 95% pollution abatement. The rate achieved by this simple organization may be sufficient to meet standards on discharge into nature, but to make water reuse viable, a tertiary disinfection treatment is needed. Microbial abatement targets up to 99.9% (3 $\log_{10}$) and obviously depends on future use of the disinfected water (vegetable/tree cultivation, greenspace irrigation, and aquifer recharge). More dramatically, today, almost 700 million people lack improved drinking water sources.[2] This is because rural areas of developing countries not equipped with sanitation and running water public network are the most affected with proliferation of many waterborne deseases.[2] In sub-Saharan areas, unsafe drinking water alone accounted for 50% of deaths.[3] Providing a simple, robust and efficient disinfection process adapted to a developing country today represents a major health issue.

Most of the time, disinfection is carried out using UVC irradiation and/or strong oxidizers such as ozone and chlorine. UVC and ozonation are efficient against most infectious agents. UVC processes involve installation, electricity, and maintenance costs. If effluent is heavily charged with organic matter, then chlorine can lead to organohalides, especially highly undesirable trihalomethanes (THMs).[4−6] Research is thus turning to alternative processes, and among those currently in development, photocatalysis is an interesting option. Photocatalysis is an environmentally friendly water disinfection technology, especially as the process can be solar-driven.[7−10] The literature has shown that photocatalysis processes can effectively inactivate a wide range of bacteria,[11,12] including *Escherichia coli*[13] which is by far the most studied organism in the world.[10,14] Nevertheless, the vast majority of such studies have been conducted using catalysts in slurries, e.g., TiO_2,[15,16] which need to be post-treated and are almost always integrated into experimental batch-type systems. These systems do not permit easy translation of results to more practical engineered treatment operations, e.g., real-world WWTPs, which inevitably work in a pseudocontinuous way.[17−20] Hence, catalysts will likely need to be immobilized on fixed support materials, and contaminated water treatment capacity should be explored and/or estimated in a continuous-flow configuration.

Within the objective to promote the direct use of solar energy to activate the photocatalytic oxidative principle, it is obviously necessary to take into account the discontinuous characteristic of the natural sunlight irradiation. This is a major constraint to manage for efficient design and running of the operating process. The large scale-up of a continuous-flow solar photocatalytic disinfection technology therefore needs a simulation tool capable of predicting how the process works

Received: September 1, 2017
Revised: November 28, 2017
Accepted: November 29, 2017
Published: November 29, 2017

DOI: 10.1021/acs.iecr.7b03644
Ind. Eng. Chem. Res. XXXX, XXX, XXX−XXX

when submitted to not just variable light flux density but also variable effluent feed flow rates.

To begin addressing some of these critical issues, the work reported here focused on the photocatalytic disinfection of Gram-negative *E. coli* in a continuous-flow operating system and using a supported catalyst implemented in a flat reactor. As far as we know, few studies have addressed continuous-flow processes,[21−23] particularly for solar disinfection purposes. The laboratory setup developed here is far from intended to replicate the complexity of actual field-scale engineered processes. However, it does enable early investigations of key parameters that will be critical to the success of larger continuous-flow solar treatment processes. As a first step, experiments were carried out to study the effect of two key parameters that govern the inactivation process: light flux density and feed flow rate. An *E. coli* inactivation simulation model was previously developed in the case of a treatment performed in batch working mode in a closed fluid loop including a cylindrical reactor.[24] As a second step, the ability of this model to represent the performances of the open reactor working in continuous flow was tested and evaluated.

2. EXPERIMENTAL SECTION

2.1. Catalyst. TiO_2 catalyst, the material most widely employed for photocatalysis, was used in an immobilized form. The photocatalytic medium (Paper Grad 1048) manufactured by Ahlstrom consisted of TiO_2 (Millenium PC-500) as a coating on nonwoven fiber. Its specific surface area, calculated with reference to the mass of the total photocatalytic medium, was 98 $m^2\ g^{-1}$. In more detail, the photocatalytic material consisted of cellulosic fibers (38 g m^{-2}), TiO_2 (16.7 g m^{-2}), and SiO_2 (13.3 g m^{-2}), where SiO_2 served as an inorganic binder for the titanium deposited on the paper fibers. This photocatalytic material has already been characterized,[25] and the major concern when using the 2D material was leaching, which may lead to a reactivity modification due to the change in TiO_2 recovery. Because of this, the media was systematically prewashed (using Milli-Q water). This prewashed media was reasonably photostable and has a TiO_2 powder recovery rate of about 20%. It is widely used and cited in the literature, and was tested, for example, for photocatalytic treatment of several organic pollutants[26] under artificial UV irradiation as well as natural sunlight.[27,28]

2.2. Bacterial Strain and Growth. *E. coli* strain DSM 30083 was used for the full bacterial inactivation study. This lab strain is widely studied, has a sequenced genome, and is a nonpathogenic primary model organism for lab research.[10,14] *E. coli* cells were grown under sterile conditions in 100 mL of Luria−Bertani (Miller's LB Broth) medium at 37 °C.[29] Bacterial growth was monitored by optical density (wavelength = 600 nm) in a spectrophotometer (UVmini-1240, Shimadzu). Cultures in stationary phase were appropriately diluted in a buffer solution (buffered sodium chloride peptone water, pH 7.0, Oxoid) in order to obtain targeted initial bacterial concentrations. For all studies, bacterial counts were monitored via MUG/*E. coli* fluorescent microplates in accordance with the requirements of standard NF EN 9308−3. Bacterial count was then evaluated in MPN L^{-1} (i.e., Most Probable Number per unit of volume).

2.3. Processing Loop. The lab setup (Figure 1) consisted of an open processing loop regarded as a perfectly mixed reactor. Its total volume of 0.25 L consisted of two parts: a photoreactor and a recirculation system linked to effluent inlet and outlet. The photoreactor was similar to a flat reactor with a parallel-piped shape, a width of 10 cm, a length of 15 cm, and a thickness of 1 cm. It had a stainless-steel base and was covered in front by a plate of UV-transparent PMMA (UV transmission equal to 90%). The photocatalytic 2D material was placed on the irradiated back face of the reactor. To isolate it from any external light source, the photoreactor was mounted within a closed chamber and exposed to a panel of UVA LED diodes (280 LEDs distributed in 10 rows, λ = 365 nm). The surface and useful volume irradiated thus obtained were 0.015 m^2 and 0.15 L, corresponding to an irradiated area per unit of volume of 10^{-4} m^2 m^{-3}. Light intensity calibration curve was established with a hemispherical UV sensor (UVA 365 Lutron Electronic Enterprise) positioned at the same place as the flat reactor surface. The PMMA reactor surface was irradiated with flux density between 3 and 50 W m^{-2}, with a small pitch of variation equal approximately to 0.2 W m^{-2} thanks to the control of the power supplied to the LED. This range of UV flux density is similar to that emitted by the solar radiation.

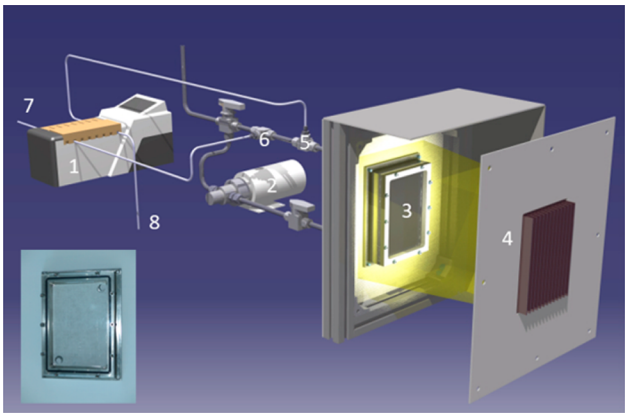

Figure 1. Processing loop: peristaltic pump (1), centrifugal pump (2), photoreactor (3), UV panel (4), withdrawal valve (5), feed valve (6), effluent to be treated (7), and treated effluent (8). Picture of the reactor with the 2D media positioned at the back face.

Fluid flow in the closed fluid loop was performed with a centrifugal pump (Cole Parmer), which ensured homogeneous mixing of the solution in the entire system that can be thus be considered a perfectly mixed reactor. In order to establish the continuous flow regime, the processing loop was fed in with the influent (bacterial suspension to be treated) at a constant flow rate. Simultaneously, the same quantity of solution was withdrawn at a same flow rate in order to keep a fixed volume of fluid into the system. The supply/withdrawal flow rates were modulated by a multichannel peristaltic pump (Watson Marlow 205 CA). Flow range was monitored between 0.01 and 0.3 L h^{-1}.

3. MODELING

A model of bacterial inactivation was built and tested[24] with success in the case of a reactor operating in a closed recirculating circuit working in batch mode. It is based on two main assumptions (that have been largely discussed elsewhere):[24] (i) A reversible adhesion of the bacteria occurs at the surface of the catalyst media; (ii) a photocatalytic reaction, consecutive to the production of hydroxyl radicals by the TiO_2 semiconductor under irradiation, likely degrades the bacteria bonded to or in the very near vicinity of the catalyst. Consequently, the couplings between bacteria mass transfer

DOI: 10.1021/acs.iecr.7b03644
Ind. Eng. Chem. Res. XXXX, XXX, XXX−XXX

from the liquid bulk to the catalyst surface, the "intrinsic" photocatalytic degradation rates, have to be taken into account in the global mass balances applied to the bacteria.

The concentration C (MPN L^{-1}) of bacteria in the liquid bulk is the result of the general mass balance including the fluid inlet and outlet as

$$V_T \frac{dC}{dt} = \dot{m}(C_{in} - C_{out}) - V_r(K_s S_{cat}(q_e - q) + \alpha I_r^f C) \quad (1)$$

The mass balance applied to bacteria bonded to the catalyst surface (q in MPN m^{-2}) leads to

$$\frac{dq}{dt} = K_s(q_e - q) - \alpha' I_r^{f'} q \quad (2)$$

where q_e (MPN m^{-2}) is bonded bacteria in equilibrium with the liquid determined experimentally[24] and approached with a Freundlich formalism:

$$q_e = 31C^{(1/0.78)} \quad (3)$$

In the balances, $\dot{m}$ is feed flow rate (L s^{-1}). V_r and V_T are the reactor and total loop volumes (L). The first term of the "disappearance" rate of the bacteria in the liquid phase in eq 1 is described according to the linear driving force (LDF) model is the flux density of bacteria transferred to the catalyst surface. It involves K_s (s^{-1}), the mass transfer coefficient expressed with the bounded phase taken as reference, and the equivalent surface of the catalyst per unit of reactor volume, S_{cat} (m^2 L^{-1}). The second part describes the photocatalytic disinfection kinetics expressed as a power function of the irradiation intensity I_r (W m^{-3}) per unit of reactor volume and involved an energy constant α ($(m^3\ J^{-1})^{-f}$), which is a function of semiconductor activity, and a coefficient f (dimensionless), which modulates the reaction rate with respect to light intensity. Similarly, the mass balances applied to the bacteria in adhesion (eq 2) involved the flux coming from the liquid phase (first term) and photodisinfection kinetics expressed according to a similar formulation with parameters α' ($(m^3.J^{-1})^{-f'}$) and f' (dimensionless).

4. RESULTS AND DISCUSSION

4.1. Preliminary Assays. The first step was to validate that the processing loop (photoreactor and circuit) may be regarded as a perfectly mixed open reactor. Loop residence time t_l was determined under dark conditions throughout the system response to a step-like input signal. This type of signal was obtained by feeding the processing loop with a tracer solution with a constant concentration and flowing at a fixed rate. In this work, *E. coli* was naturally selected as the tracer. Bacterial concentrations at the exit stream of the process over time were monitored. Prior to the start of the experiment, the processing loop was fully filled with an initial *E. coli* bacterial suspension charged at a concentration C_0 of 10^5 MPN L^{-1}. For better accuracy, two step-like input signals were successively applied: a first "high" input signal, and a second "low" one. After an initial lag phase (10 h), the loop was first supplied with a bacterial suspension of a concentration $C_{in,1}$ of 1.510^7 MPN L^{-1} (150 times more concentrated than C_0) at a flow rate $\dot{m}$ of 0.06 L h^{-1} (Figure 2). The exit-stream bacterial concentration C_{out} was monitored over time until reaching steady state, i.e., until reaching a stable concentration identical to that of the inlet stream ($C_{in,1} = C_{out}$). A second concentration gap was applied.

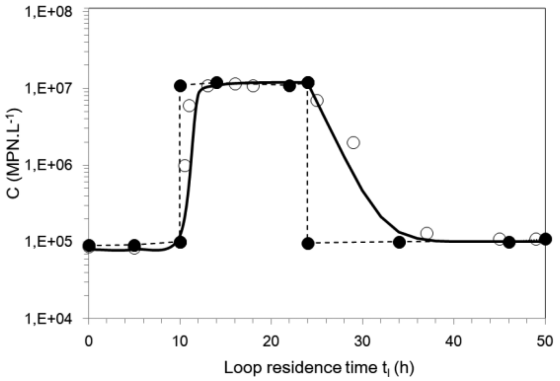

Figure 2. Experimental (○) and simulated (continuous line) bacterial concentrations in the exit stream of the processing loop for an input step-like signal. Experimental measures of bacterial concentrations in the feed stream (●).

The processing loop at an initial concentration $C_0 = C_{in,1}$ was supplied with a second bacterial suspension flowing at a same flow rate (0.06 L h^{-1}) but of a concentration $C_{in,2}$ of 10^5 MPN L^{-1} (150 times more diluted than $C_{in,1}$).

The response of a perfectly mixed open reactor to such a signal may be expressed following the general formulation of eq 1, and obviously corresponds to the special case where no photocatalyst is loaded and when irradiation is off, i.e., with no reaction taking place. The integration of eq 1 for each step leads to

$$C_{out}(t) = C_{in} - (C_{in} - C_o)\exp(-t/t_l) \quad (4)$$

where $t_l = V_T/\dot{m}$ (s) is loop residence time and C_0 is initial concentration of the step considered.

Time-course profiles of the calculated and experimentally measured bacterial concentrations in the exit stream of the processing loop were plotted in Figure 2. The best agreement between calculated and experimental concentration profiles was for a residence time of $t_l = 4$ h, to be compared against 4.16 h in the case of a perfect mixed open reactor. This corresponded to a dead volume of 9 mL (while the loop volume is of 250 mL), which was considered negligible for further study.

For the second preliminary assays, the experiments were performed both in presence and absence of the catalyst. In both cases, concentration profiles were expressed as a function of reactor residence time ($t_r = V_r/\dot{m}$), time of irradiation, and the representative time of bacteria-to-catalyst contact (when present). The starting of the assays was first carried out under dark conditions (Figure 3) for t_r between 0 and 30 h. The photocatalytic media appeared to initially slow the increase of the bacterial concentration in the exit stream. This was probably a consequence of transfer then adhesion of the bacteria from the liquid phase to the catalyst surface. Once the steady state was reached, bacterial concentration in the exit stream was identical to that of the inlet stream, which suggests a balanced state of bacteria between the catalyst surface being fully loaded of cells and the liquid bulk. This made it possible to experimentally illustrate the "adhesion effect" of the material on the bacteria. Under light conditions, bacterial disinfection obtained by photolysis and photocatalysis were clearly distinguished. Both profiles decreased exponentially and then stabilized within 8 and 11 h, respectively, of irradiation. While the share attributable to the direct bactericidal action of light

DOI: 10.1021/acs.iecr.7b03644
Ind. Eng. Chem. Res. XXXX, XXX, XXX−XXX

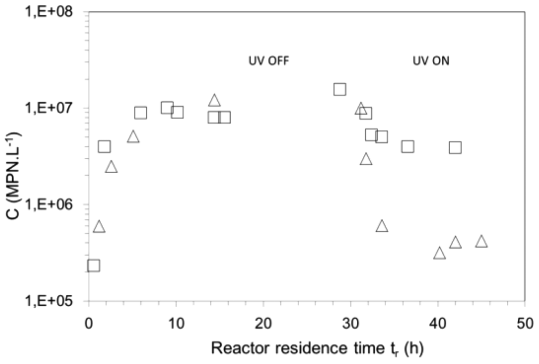

Figure 3. Experimental bacterial concentration profiles at the outlet of the process for a feed flow rate of 0.025 L h^{-1} and at inlet concentration C_{in} = 1 × 10^7 MNP L^{-1} without (□) and with (△) photocatalytic media. Dark conditions between 0−30 h followed by photolysis (□) or photocatalysis (△) with a light flux density at the reactor surface equal to 35 W m^{-2}.

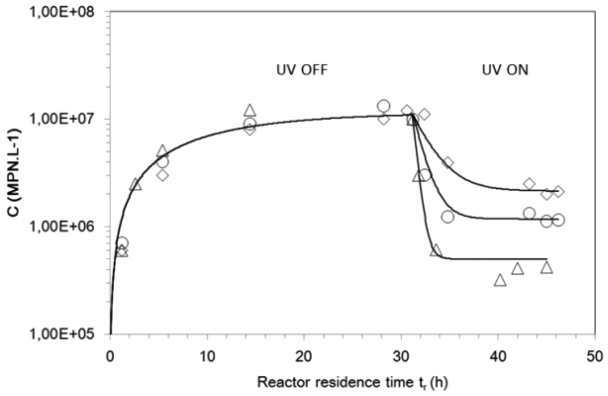

Figure 4. Experimental and simulated time-course of bacterial concentrations in the exit stream of the process for a fixed feed flow rate of 0.025 L h^{-1} and at inlet concentration C_{in} = 1 × 10^7 MNP L^{-1}. Dark conditions followed by photocatalysis with light flux densities of 10 W m^{-2} (◇), 20 W m^{-2} (○), and 35 W m^{-2} (△).

was not fully negligible, it nevertheless remained far lower than that of photocatalysis, which is consistent with the literature.

4.2. Light Flux Density Effect. Irradiation level is a key parameter in characterizing the photocatalytic disinfection process. The influence of flux density in the heterogeneous photocatalysis disinfection process has been widely reported,[30−32] but most of these studies were conducted in batch systems where residence time in the reactor was ultimately not a limiting factor for effective inactivation of the bacteria. In contrast to the batch system, the disinfection of bacteria in an open system takes place in a single pass. In this case, the control of the irradiation conditions in the reactor becomes critical to effective abatement of the cells. Our aim was therefore to evaluate the irradiation effect on the bacteria in the open reactor and assess the capacities of the photocatalytic treatment for population reduction, particularly in steady state.

Under dark conditions, the processing loop without any bacteria (At t_r = 0, C_0 = 0 MPN L^{-1}) was filled with a bacterial suspension charged at 10^7 MPN L^{-1}. Feed flow rate was fixed at 0.025 L h^{-1} and held constant throughout the experiment. After at least 25 h, when the outlet concentration profile met the value of the inlet concentration (equilibrium was reached between bacteria in adhesion and in liquid phase), the experiments were next led under controlled light flux density. The photocatalytic tests were investigated under irradiation flux densities at the surface of the reactor of 10, 20, and 35 W m^{-2}. Time-course of bacterial concentration was monitored periodically in the exit stream of the processing loop. The results obtained are shown in Figure 4.

As expected, during the first phase, under dark conditions when the bacterial concentrations in the loop increase, the curves corresponding to the three assays overlap. The bacteria concentration profiles during this step only depend on the loop residence time and the initial condition, both of which were identical for the three assays. The good agreement between experimental measures substantiated a decidedly good reproducibility of the assays.

During the irradiation phase, the curves obtained also depicted two regimes, i.e., a first regime where bacterial concentrations decreased, and a second regime representing the steady state. This latter scheme corresponded, as for any perfectly mixed open reactor, to the balance between the inlet and outlet steam of bacteria in the system and the "photocatalytic reaction", i.e., the disinfection effect, taking place in the reactor under irradiation. Relatively to the respective light flux densities studied, when the steady states were reached, the corresponding bacterial abatements achieved were 80, 89, and 96%. A decisive advantage of working to a permanent regime is to have direct access to the disinfection-rate values thanks to eq 1, i.e., 13 × 10^5, 14.7 × 10^5, and 16 × 10^5 MPN h^{-1} L^{-1} for 10, 20, and 35 W m^{-2}, respectively. Even if the effect is moderated, as expected, then results showed that the disinfection rates increased with light flux density. This confirms the dependency of bacterial disinfection on amount of irradiation, i.e., a specific link between the amounts of photons received in the reactor and the production of the radical species responsible for the photocatalytic reaction (oxidative action).[19,33] The experiments also demonstrate that in the case of a 2D media probably because of the mass transfer limitation and/or the light saturation of the photocatalytic sites the photons efficiency dramatically decreases with increasing intensity. The photons flux is directly proportional to the level of intensity and at a wavelenght of 365 nm (UV LED panel) 1 J s^{-1} corresponds to 3 μmol s^{-1} of photons, but the experimental rate of the bacteria inactivation is far from being proportional to the light flux density.

4.3. Feed Flow Rate Effect. Next, experiments were carried out to assess the influence of the flow rate conditions. As previously, the processing loop was charged initially with a bacterial suspension at 10^7 MPN L^{-1}. The feed flow rates studied were 0.06, 0.04, and 0.025 L h^{-1}. As previously, the experimental tests were initiated in the dark then conducted under a constant UV light flux density at the reactor surface of 35 W m^{-2}. Figure 5 shows the results of the bacterial concentrations measured in the exit stream for the variable feed flow rates.

Under dark conditions, the increase in bacterial concentration was obviously highly dependent on feed flow rate. Residence time decreased as flow rate increased. Relatively to the respective feed flow rates applied, the residence time values obtained were 4.16, 6.25, and 10 h, which are values of comparable amplitude to those of classic treatment plants (biological treatment).

As previously, under irradiation, the bacterial profiles depicted two regimes: a first transitory regime, and a second steady state. Both regimes were strongly dependent on feed

DOI: 10.1021/acs.iecr.7b03644
Ind. Eng. Chem. Res. XXXX, XXX, XXX−XXX

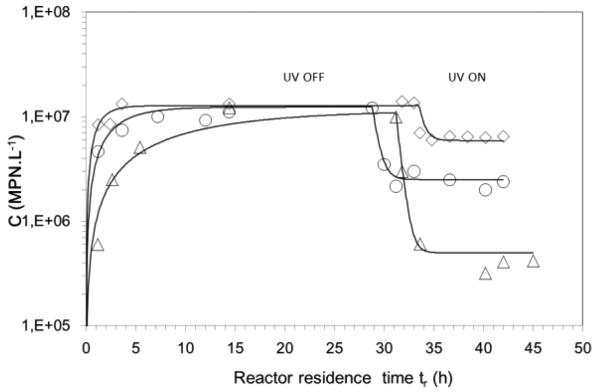

Figure 5. Experimental and simulated time-course of bacterial concentrations in the exit stream of the process for a fixed light flux density of 35 W m^{-2} and at inlet concentration C_{in} = 1 × 10^7 MNP L^{-1}. Dark conditions followed by photocatalysis with feed flow rates equal to 0.06 L h^{-1} (◇), 0.04 L h^{-1} (○), 0.025 L h^{-1} (△).

flow conditions. The relative bacterial concentration reductions achieved for flow rates of 0.06, 0.04, and 0.025 L h^{-1} were assessed at 37, 76, and 96%, respectively, but corresponded to bacterial disinfection rates of around 30 × 10^5, 22 × 10^5, and 16 × 10^5 MPN h^{-1} L^{-1}, respectively. These results clearly showed that high concentrations maintained in the loop in high-flow-rate cases were conducive to high rate of treatment.

Residence time and therefore feed flow condition as well as irradiation intensity appeared to be major factors to be taken into account to properly meet the treatment objectives. Therefore, finding the right trade-off between all factors would be the best way to guarantee the optimal treatment yield. This further demonstrates the great need for a mathematical tool that would be able to predict disinfection performance while taking into account the different hydrodynamic characteristics of the reactor, the catalyst surface, and the various key parameters on which the process depends. This is particularly relevant within an objective of a direct use of the solar energy that is naturally discontinuous. In this case, the validation of a simulation tool able to be representative of the treatment capacities under different irradiation levels (and in transient regime) only represents the first step. The second bottleneck to overcome, not taken into consideration in this paper, will be to implement a storage function able to manage the discontinuity of the ressource. Among the different options, hybridation between photocatalysis and sorption is probably one of the most promising.[34,35]

5. PHOTOCATALYTIC TREATMENT SIMULATION

Apart from the experimental conclusions obtained, the objective of the study was to obtain the values of the unknown parameters involved in the mass balances that best reproduce the experimental photocatalytic results. The model summarized in the previous section was based on the coupling between two distinct phenomena.

The first phenomenon is the transfer of bacteria from the solution to the surface of the catalyst, which involves equilibrium conditions between bacteria in adhesion and bacteria in the bulk phase, and a mass transfer coefficient K_s. In a fully developed laminar regime, the regime corresponding to the flow conditions of the experiments performed in this work and in the batch working mode of the previous set of experiments, K_s can be considered of the same order of magnitude,[22] its value was set to 2.16 × 10^{-6} s^{-1}. Likewise, the equilibrium condition $q_e = 31C^{(1/0.78)}$ has to be independent of the processing loop. Under dark conditions, these "assumptions" are validated by the comparison of the experimental bacterial concentrations in the liquid phase and the simulated concentrations obtained by the resolution of the set of differential equations for the three different fluid flow conditions (Figures 4 and 5). For each case with C and q set equal to 0 at the initial time, the model was able to translate the working of the process in the presence of the catalyst, whatever the flow conditions. The model successfully managed to reproduce the progressive accumulation of bacteria in the reactor, all while taking into account the bacterial adhesion phenomenon. Obviously, the model described the subsequent state of balance that took place between the flux of bacteria fed into the reactor and the catalyst surface being in equilibrium with the liquid bulk.

Under irradiation, the second phenomenon that enters into play and happens simultaneously to bacteria transfer is the photocatalytic disinfection reactions. It is expressed as a function of bacteria concentration in the liquid phase (C), bacteria in adhesion (q), and power functions of the irradiation intensity I_r (W m^{-3}) involving several kinetic coefficients, i.e., α ($(m^3\ J^{-1})^{-f}$), α' ($(m^3\ J^{-1})^{-f'}$), f, and f' (dimensionless). Ideally, these coefficients have to be fully independent of reactor geometry, size, and closed or open working mode. Nevertheless, under irradiation, the values of α, α', f, and f' were optimized to provide the best fit to the new set of data obtained. The parameters were identified using an optimization method (optimization via Matlab) based on the minimization of the mean relative error (MRE) following

$$\mathrm{MRE}\ (\%) = \frac{1}{n}\sum_{i=1}^{n}\left|\frac{(C_{exp} - C)}{C_{exp}}\right| \times 100 \quad (5)$$

where C and C_{exp} are the bacterial concentration values predicted by the model and the experimental data, respectively, and n is number of data points. Table 1 reports the kinetic parameters identified. Following this optimization process, calculations were performed with the same values of the kinetic parameters, regardless of the operating conditions. Under irradiation, even though deviations were observed, the simulated results obtained under variable light flux densities I_r (Figure 4) and feed flow rates (Figure 5) fitted with a reasonable degree of accuracy (MRE = 20.2%) to the experimental bacterial concentration measures in both transitory and steady-state regimes. The kinetic model was successfully able to describe the overall approach based on the description of the disinfection process in the liquid as well as in the solid phase. This confirmed, accordingly, that bacterial

Table 1. Optimized Mass Transfer and Kinetic Parameters Involved in the Models

coefficient mass transfer − kinetic	continuous mode (this study)	batch mode[24]
K_s (10^{-6} s^{-1})	2.16	2.16
α (10^{-6} m^3J^{-1})$^{-f}$	4.1	10.2
α' ($10^{-6}m^3J^{-1}$)$^{-f'}$	1.6	19.4
f	1.39	1.2
f'	0.093	0.064
MRE (%)	20.2	9.8

DOI: 10.1021/acs.iecr.7b03644
Ind. Eng. Chem. Res. XXXX, XXX, XXX−XXX

reduction in the fluid bulk and especially in the steady state is definitely governable by the two main phenomena previously described: bacterial transfer to the catalyst surface and the photocatalytic reaction rate dependent on the quantity of energy absorbed into the photoreactor.

Ideally, the concentration profiles should be simulated with the same set of parameters whatever the working mode of the reactor, i.e., batch mode or continuous mode (Table 1). This is indeed the case for the mass transfer coefficient (K_s), but differences emerge for the other kinetic coefficients. Note however that the set of kinetic parameters remains of very similar order of magnitude. It is also interesting to underline that it is mainly the kinetic constant α', characteristic of the inactivation of bacteria in adhesion to the surface of the catalyst, that differs from one type of experiments to another. The coefficient α' differs by a factor of 10 when switching from batch to permanent operation, whereas the kinetic constant α differs by a factor of around two. Although the operating conditions are radically different in both cases, i.e., transient versus permanent regime, cylindrical versus Cartesian geometry, the initial conditions (in particular, the initial state of the catalyst surface) are probably the most marked differences between the two types of experiments. In batch experiments, the catalyst surface is initially free of bacteria and is rapidly charged at the start of treatment. However, in the steady-state experiments, when irradiation is delivered, the catalyst surface is in equilibrium with the liquid phase and saturated with bacteria. Under irradiation, the density of bacteria at the catalyst surface decreased dramatically at the beginning of the experiment; this is due to the inactivation of bacteria on the surface or in the very near vicinity of the catalyst. Thus, it is probably the assumption of a perfect reversibility of the phenomenon of adhesion (implicit in the adopted formalism) which is partly at fault. Considering that the inactivated bacteria are systematically or immediately released to the liquid phase certainly leads us to overestimate the role played by the surface of the catalyst in the overall inactivation process. On this basis, which should probably be supported by additional tests, it is *a priori* the results from the experiments carried out with the process operating in continuous mode and leading to a steady state that makes it possible to best approach the reality of a disinfection process.

6. CONCLUSION

In this work, we developed a flat-plate open reactor irradiated with an LED panel that made it possible to study photocatalytic inactivation of the target bacteria *E. coli*. Depending on the initial conditions, with a continuous feed flow and a constant irradiation, the system designed allow to study phenomena in transient as well as steady-state or permanent working mode. In the case of permanent regime, a decisive advantage is a direct access to the experimental inactivation-rate values via a simple mass balance between inlet and outlet. The small scale-up pilot facilitated preliminary investigation of the key factors governing the continuous flow water disinfection system, i.e., light flux density and feed flow rate. At around 35 W m^{-2}, a level of irradiation in the range of solar UV, the experimentally determined treatment capacity of the selected 2D media is in the range of $15-30 \times 10^5$ MPN h^{-1} L^{-1}.

Beside experimental investigations, the second objective was to build on a study undertaken in a previous work a representative model for open reactors operating in continuous mode for photocatalytic inactivation of *E. coli*. The model is based on coupling the mass transfer between bacteria in the liquid bulk phase and bacteria in "adhesion" at the surface of the photocatalytic media and the inactivation of *E. coli* at different rates in both phases. After an optimization procedure, the model was successfully compared to the experimental data. It is able to reproduce the evolution in concentrations of viable bacteria in the range of UV flux densities corresponding to solar irradiation and at variable feed flow rates of comparable amplitude to those applied in real-world wastewater treatment plants. Finally, we anticipate this model to be a starting point for the development of a numerical tool for scaling up efficient photocatalytic open reactors using immobilized photocatalytic media and operating under sunlight. This would then offer the possibility to predict process capacities under a dynamic flow regime, as a function, for example, of irradiation availability (weather, daily cycles, and geographic location) and to meet, for example, given operational constraints or objectives, e.g., percentage of abatement, treatment of a given water volume, and so on.

AUTHOR INFORMATION

Corresponding Author

*E-mail: vincent.goetz@promes.cnrs.fr.

ORCID

Vincent Goetz: 0000-0001-5700-6487

Notes

The authors declare no competing financial interest.

ACKNOWLEDGMENTS

We thank G. Hernandez, R. Garcia, and J. J. Huc for their help in designing and building the demonstrator. This work was supported by the Programme "Investissements d'avenir" (Investment for the Future) of the Agence Nationale de la Recherche (National Agency for Research) of the French State under award number ANR-10-LABX-22-01-SOLSTICE. It was also supported by the regional project "Chercheur d'Avenir".

REFERENCES

(1) *The United Nations World Water Development Report: Wastewater the Untapped Resource*; UNESCO: Paris, 2017.

(2) *Progress on Sanitation and Drinking Water-2015 Update and MDG Assesment*; WHO/UNICEF: Geneva, Switzerland, 2015.

(3) Prüss-Ustün, A.; Bartram, J.; Clasen, T.; Colford, J. M.; Cumming, O.; Curtis, V.; Bonjour, S.; Dangour, A. D.; De France, J.; Fewtrell, L.; Freeman, M. C.; Gordon, B.; Hunter, P. R.; Johnston, R. B.; Mathers, C.; Mäusezahl, D.; Medlicott, K.; Neira, M.; Stocks, M.; Wolf, J.; Cairncross, S. Burden of disease from inadequate water, sanitation and hygiene in low- and middle-income settings: a retrospective analysis of data from 145 countries. *Trop. Med. Int. Health* **2014**, *19*, 894.

(4) Coleman, H. M.; Marquis, C. P.; Scott, J. A.; Chin, S. S.; Amal, R. Bactericidal effects of titanium dioxide-based photocatalysts. *Chem. Eng. J.* **2005**, *113*, 55.

(5) Yang, X.; Shang, C.; Westerhoff, P. Factor affecting formation of haloacetonitriles, haloketones, chloropicrin and cyanogen halides during chloramination. *Water Res.* **2007**, *41*, 1193.

(6) Guo, Z.; Lin, Y.; Xu, B.; Hu, C.-Y.; Huang, H.; Zhang, T.-Y.; Chu, W.-H.; Gao, N.-Y. Factor affecting THM, HAN and HNM formation during UV-chlor(am)ination of drinking water. *Chem. Eng. J.* **2016**, *306*, 1180.

(7) Pham, H. N.; McDowell, T.; Wilkins, E. Photocatalytically mediated disinfection of water using TiO2 as a catalyst and spore forming Bacillus Pumulus as a model. *J. Environ. Sci. Health, Part A: Environ. Sci. Eng. Toxic Hazard. Subst. Control* **1995**, *30*, 627.

DOI: 10.1021/acs.iecr.7b03644
Ind. Eng. Chem. Res. XXXX, XXX, XXX−XXX

(8) Block, S. S.; Seng, V. P.; Goswami, D. W. Chemically enhanced sunlight for killing bacteria. *J. Sol. Energy Eng.* **1997**, *119*, 85.
(9) Bekbölet, M.; Balcioglu, I. Photocatalytic degradation kinetics of humic acid in aqueous TiO2 dispersions: The influence of hydrogen peroxide and bicarbonate ion. *Water Sci. Technol.* **1996**, *34*, 73.
(10) Malato, S.; Fernandez-Ibanez, P.; Maldonado, M. I.; Blanco, J.; Gernjak, W. Decontamination and disinfection of water by solar photocatalysis: Recent overview and trends. *Catal. Today* **2009**, *147*, 1.
(11) Otaki, M.; Hirata, T.; Oghaki, S. Aqueous microorganisms inactivation by photocatalytic reaction. *Water Sci. Technol.* **2000**, *42*, 103.
(12) Sichel, C.; Tello, J.; de Cara, M.; Fernandez-Ibanez, P. Effect of UV solar intensity and dose on the photocatalytic disinfection of bacteria and fungi. *Catal. Today* **2007**, *129*, 152.
(13) Kacem, M.; Bru-Adan, V.; Goetz, V.; Steyer, J. P.; Plantard, G.; Sacco, D.; Wéry, N. Inactivation of Escherichia coli by TiO2-mediated photocatalysis evaluated by a culture method and viability-qPCR. *J. Photochem. Photobiol., A* **2016**, *317*, 81.
(14) McCullagh, C.; Robertson, J. M. C.; Bahnemann, D. W.; Robertson, P. K. J. The application of TiO2 photocatalysis for disinfection of water contaminated with pathogenic micro-organisms: a review. *Res. Chem. Intermed.* **2007**, *33*, 359.
(15) Gumy, D.; Morais, C.; Bowen, P.; Pulgarin, C.; Giraldo, S.; Hajdu, R.; Kiwi, J. Catalytic activity of commercial of TiO2 powders for the abatement of the bacteria (E. coli) under solar simulated light: influence of the isolectric point. *Appl. Catal., B* **2006**, *63*, 76.
(16) Blanco-Gálvez, J.; Fernández-Ibáñez, P.; Malato-Rodríguez, S. Solar photocatalytic detoxification and disinfection of water: recent overview. *J. Sol. Energy Eng.* **2007**, *129*, 4.
(17) Matsunaga, T.; Tomoda, R.; Nakajima, T.; Nakamura, N.; Komine, T. Continuous-sterilization system that uses photosemiconductor powders. *J. Appl. Environ. Microbiol.* **1988**, *54*, 1330.
(18) Gill, L. W.; McLoughlin, O. A. Solar disinfection kinetic design parameters for continuous flow reactors. *J. Sol. Energy Eng.* **2007**, *129*, 111.
(19) Pal, A.; Pehkonen, S. O.; Yu, L. E.; Ray, M. B. Photocatalytic inactivation of airborne bacteria in a continuous-flow reactor. *Ind. Eng. Chem. Res.* **2008**, *47*, 7580.
(20) Dalrymple, O. K. *Mechanistic modeling of photocatalytic water disinfection*, Ph.D. Thesis, South Florida University, Tampa, FL, 2011.
(21) Farooq, S.; Engelbrecht, R. S.; Chian, E. S. K. Influence of temperature and U.V. light on disinfection with ozone. *Water Res.* **1977**, *11*, 737.
(22) Roy, D.; Chian, E. S. K.; Engelbrecht, R. S. Kinetics of enteroviral inactivation by ozone. *J. Environ. Eng. Div. (Am. Soc. Civ. Eng.)* **1981**, *107*, 887.
(23) Kouame, Y. *CSTR Microbial inactivation by free and combined chlorine*, Ph.D. Thesis, Illinois Institute of Technology, Chicago, IL, 1990.
(24) Kacem, M.; Goetz, V.; Plantard, G.; Wery, N. Modeling heterogeneous photocatalytic inactivation of E.coli using suspended and immobilized TiO2 reactors. *AIChE J.* **2015**, *61*, 2532.
(25) Correia, F. *Experimental study and modeling of solar photochemical reactor: photocatalytic media performances*, Ph.D. Thesis, UPVD, Perpignan, France, 2011.
(26) Lhomme, L.; Brosillon, S.; Wolbert, D. Photocatalytic degradation of pesticides in pure water and a commercial agricultural solution on TiO2 coated media. *Chemosphere* **2008**, *70*, 381.
(27) Janin, T.; Goetz, V.; Plantard, G.; Brosillon, S. Solar photocatalytic mineralization of 2,4-dichlorophenol and mixtures of pesticides: kinetic model of mineralization. *Sol. Energy* **2013**, *87*, 127.
(28) Goetz, V.; Cambon, J. P.; Sacco, D.; Plantard, G. Modeling aqueous heterogeneous photocatalyticdegradation of organic pollutants with immobilized TiO2. *Chem. Eng. Process.* **2009**, *48*, 532.
(29) Pigeot-Remy, S.; Simonet, F.; Errazuriz-Cerda, E.; Lazzaroni, J. C.; Atlan, D.; Guillard, C. Photocatalysis and disinfection of water: Identification of potential bacterial targets. *Appl. Catal., B* **2011**, *104*, 390.
(30) Wei, C.; Lin, W.; Zainal, Z.; Williams, N.; Zhu, K.; Kruzic, A. P.; Smith, R. L.; Rajeshwar, K. Bactericidal activity of TiO2 photocatalyst in aqueous media: toward a solar- assisted water disinfection system. *Environ. Sci. Technol.* **1994**, *28*, 934.
(31) Rincón, A. G.; Pulgarin, C. Photocatalytical inactivation of E.coli: effect of (continuous−intermittent) light intensity and of (suspended−fixed) TiO2 concentration. *Appl. Catal., B* **2003**, *44*, 263.
(32) Cho, M.; Chung, H.; Choi, W.; Yoon, J. Linear correlation between inactivation of E.coli and OH radical concentration in TiO2 photocatalytic disinfection. *Water Res.* **2004**, *38*, 1069.
(33) Goswami, D. Y.; Trivedi, D. M.; Block, S. S. Photocatalytic disinfection of indoor air. *J. Sol. Energy Eng.* **1997**, *119*, 92.
(34) Goetz, V.; Janin, T.; Plantard, G.; Brosillon, S. Hybridation between heterogenousphotocatalysis and adsorption. *Int. J. Eng. Pract. Res.* **2013**, *2*, 86−93.
(35) Yap, P. S.; Lim, T. T. Solar regeneration of powdered activated carbon impregnated with visible-light responsive photocatalyst: Factor affecting performances and predictive model. *Water Res.* **2012**, *46*, 3054−3064.

DOI: 10.1021/acs.iecr.7b03644
Ind. Eng. Chem. Res. XXXX, XXX, XXX−XXX